The Blackfoot 3C-3D seismic survey: A case study

Gary F. Margrave, Don C. Lawton, Robert R. Stewart, Susan L.M. Miller, Grace Y.C. Yang, Vladan Simin, Colin C. Potter, Qi Zhang and Todor Todorov

SUMMARY

A 3C-3D seismic survey was acquired over a Lower Cretaceous incised channel filled with porous cemented sand or possibly shale. Dipole sonic logs reveal the sand-filled channel has an anomalously low v_p/v_s ratio (or Poisson's ratio) relative to the shale-fill or to regional stratigraphy. Buried (18 m) explosive sources were recorded into a patch of 3C geophones and the data was processed to yield two independent migrated volumes representing P-P and P-S primary reflections. Isochron maps from both volumes were combined algebraically to yield maps of the v_p/v_s ratio which delineate the channel much better than is possible with P-P data alone. The channel also shows a strong P-P AVO anomaly which is spatially correlated with the v_p/v_s ratio anomaly.

INTRODUCTION

A 3C-3D seismic survey was acquired over the Blackfoot field (near Strathmore, Alberta, Canada) in 1995. The survey was sponsored by a group of Calgary based exploration companies and was planned and conducted by the CREWES Project and Boyd Exploration Consultants. (See Stewart et al., 1996, for more information.) Simultaneously with the surface data acquisition, a 5-level 3C downhole tool (Western Atlas) was deployed in a well and a 3C-3D VSP was recorded.

The producing formation is a cemented channel sand (the Lower Cretaceous Glauconitic, Figure 1) deposited as incised valley-fill sediments just above the Mississippian carbonates (Wood and Hopkins 1992). The Glauconitic sandstone is up to 35 m thick and is approximately 1550 m below surface in the Blackfoot area. Average porosity is near 18% in the producing sandstone and cumulative production throughout southern Alberta exceeds 200 MMbbls oil and 400 BCF gas (Miller et al., 1995).

GEOPHYSICAL CONSIDERATIONS

The primary seismic imaging objectives were delineating the channel boundaries and distinguishing sand-filled from shale-filled channel. Conventional (single component) seismic data has been less successful than desired in addressing these goals. Especially problematic has been the discrimination of sand-filled from shale-filled channel.

Dipole sonic information from 3-wells (a sand-filled channel well, a shale plugged channel well, and a regional well) indicate that the sand-filled channel has an anomalously low Poisson's ratio of ~.21 compared to ~.3 for the other two wells. Thus, it is expected that the estimation of Poisson's ratio, or equivalently the v_p/v_s ratio, from seismic data will provide a valuable discriminator.

Conventional (P-P) seismic data can provide v_p/v_s estimates through AVO amplitude analysis. The 3C-3D seismic survey was acquired to demonstrate that v_p/v_s ratios can also be obtained in a completely independent fashion through the joint traveltime analysis of P-P and P-S data volumes. For this purpose, conventional buried (18 m) explosive sources were recorded into a patch of 3C phones. The design of the source and receiver lines used P-S and P-P raytracing considerations to ensure good population of CMP and CCP (common conversion point) bins (Cordsen and Lawton, 1996). The resulting 3-C data were processed for both P-P and P-S primary reflections to produce two independent 3-D migrated volumes. Figure 2 shows a segment of the final P-P and P-S data in section display. Since P-S travel times are roughly 1.5 times larger than P-P times, the P-S is plotted at a compressed time scale relative to P-P. Final signal bandwidths were 10-80 Hz for P-P and 10-40 Hz for P-S. As plotted in Figure 2, the two datasets have similar resolution and interpretability.

INTERPRETATION

The interpretation was guided by P-P and P-S synthetic seismograms created from the available dipole sonic and density log information. For each well, a densely layered model was created and an elastic wave modeling technique (Lawton and Howell, 1992) was used to create synthetic P-P and P-S offset gathers. (Only primary reflections were considered in these simulations.) The gathers were then stacked to simulate fully migrated images. The resulting P-P and P-S synthetic seismograms, with known formation boundaries, were then compared with the data volumes to establish wavelet phase and to determine picking criteria for the events of interest.

Interpretation proceeded by picking and mapping a number of events, in both data volumes, above and below the channel interval including (in order from shallow to deep): Viking, Mannville, Lower Mannville, top channel, Mississippian, Wabamun, and Cambrian. A serious complication is the "picking mismatch" which refers to the fact that it is not generally possible to ensure that picks in the P-P volume correspond to the same depths as picks in the P-S volume. This is a consequence of: the P-P volume has roughly twice the signal band (in temporal frequency) of the P-S volume, the S wave velocities are about half the P-wave velocities, and the P-P and P-S reflectivities are distinctly different. Thus, the two data volumes have different resolution in depth and exhibit distinctly different tuning phenomena. The roughly 30 m thick Glauconite channel is below tuning on both datasets. Since seismic picks generally follow a distinct waveform feature (peak, trough, zero crossing, etc.) it is unlikely that P-P and P-S picks will coincide in depth.

Interpretation can then proceed along the usual lines for both the P-P and P-S datasets. (See Lawton et al., 1997, for more information.) Time and depth structures can be mapped and isochron and isopach maps can be constructed by the usual differencing. Figure 3 shows a time slice through the Channel interval on the P-P volume (flattened on the Wabamun which is about 100 ms below the Mississippian) while Figure 4 is a similar slice through the P-S volume. The Channel trend runs from south to north along the western half of the survey and is denoted approximately by the arrows and the black dots representing producing oil wells. A common exploration technique is to pursue P-P amplitude bright spots (large negative amplitudes); but, as Figure 3 shows there are many false correlations. The P-S time slice through the channel interval gives a much better indication though the brightest amplitudes are displaced about 100-200 m westward from the producing well trend.

Current practice is to build P-P and P-S interpretations independently though it is obviously more desirable to use both to constrain a single depth interpretation. The construction of v_p/v_s ratio maps is a step in this direction in that isochron maps from both volumes are involved according to the formula (Garotta et al., 1987):

$$v_p / v_s = \frac{2\Delta t_{ps} - \Delta t_{pp}}{\Delta t_{pp}} \quad (1)$$

where Δt_{ps} and Δt_{pp} are the P-S and P-P isochron maps for a particular interval. A consequence of the picking mismatch mentioned earlier is that these v_p/v_s ratios will often be numerically unrealistic though they still show valid relative changes along the stratigraphy.

The most definitive interpretation product was the v_p/v_s ratio over the Channel-Wabamun interval. The Wabamun is a strong, easily mapped reflector about 100 ms beneath the Mississippian. The Channel-Wabamun interval was chosen rather than the Channel-Mississippian because the Mississippian is very difficult to pick consistently in either data volume. Under the reasonable assumption that the sand-filled channel is the only significant formation with an anomalous v_p/v_s ratio in this interval, this should still be a diagnostic choice. Figure 5 is the v_p/v_s ratio map created from P-P and P-S isochron maps using equation 1. The arrow indicates the obvious anomaly trending parallel to the producing wells but with the mentioned westward displacement of about 150 m. The lowest v_p/v_s ratios are about 1.5 which corresponds to a Poisson's ratio of about .1 which is somewhat lower than indicated in logging. This is likely an effect of the picking mismatch. Note that all producing wells are indicated by v_p/v_s ratios of less than 1.8 and all dry holes have ratios greater than 1.8.

Figure 6 shows an estimation of the P-P AVO anomaly associated with the channel. For this purpose, the P-P prestack data was divided into near offsets (0 - 900 m) and far offsets (1200 - 2100 m). These subsets were then stacked, signal enhanced, and 3D migrated. Figures 6A and 6B are near and far offset time slices through the Channel and Figure 6C is their difference. Though we do not present an inversion of the AVO for the v_p/v_s ratio, it is obvious from comparison with Figure 5 that the AVO anomaly is spatially correlated with the v_p/v_s ratio anomaly.

Both anomalies are offset ~150 m to the west of the trend of producing wells. The very different computation procedures for these anomaly maps argues that this is a real, physical effect. It seems likely that the sweet-spot of the channel is displaced to the west. The wells were all drilled on P-P amplitude trends like those shown in Figure 3 which do not predict the v_p/v_s ratio anomaly.

Figure 7 is an estimation of the "fractional percentage shale" as computed by cokriging of gamma ray log data and the v_p/v_s ratio map. It is an illustration one of the many supplemental products which can be created from 3C-3D data.

Figure 8 shows a result from the 3C-3D VSP. As the survey was being recorded, it proved impossible to coordinate tool depth with source position. Consequently, the tool was simply raised and lowered "randomly" resulting in a very irregular geometry. Though this complicated processing, good results were obtained which compared quite well with surface data and synthetics.

Finally, we mention that we cannot yet prove that the anomalies detected were not production induced. We are confident that they represent the current physical state of the reservoir but cannot be sure that they would be present in a virgin Glauconitic setting. However, we note that the dipole sonic information, which was collected shortly after drilling, predicts these anomalies and supports the notion that these effects were not caused by production.

CONCLUSIONS AND COMMENT

Seismic 3C-3D recording is a viable technique which results in two independent data volumes representing P-P and P-S information. It is especially useful in providing v_p/v_s ratio (or Poisson's ratio) information. In conventional P-P AVO analysis, v_p/v_s ratios are estimated from an inversion of the amplitude with offset trend. In contrast, 3C-3D data allows this information to be computed directly from conventional traveltime analysis.

We estimate the cost of acquisition, processing and interpretation of a 3C-3D to be about 30-40% higher than a conventional 1C-3D of similar fold.

ACKNOWLEDGMENTS

We thank the sponsors of the Blackfoot 3C-3D group shoot and the Sponsors of the CREWES Project for their support.

REFERENCES

Cordsen, A., and Lawton, D.C., 1996, Designing 3-component 3D seismic surveys: Expanded Abstracts, 66th Annual Meeting of the Society of Exploration Geophysicists, Denver

Garotta, R., Marechal, P., and Megesan, M., 1985, Two-component acquisition as a routine procedure for recording P-waves and converted waves: Journal of the Canadian Society of Exploration Geophysicists, **21**, 40-53.

Lawton, D.C., and Howell, T.C., 1992, P-P and P-SV synthetic stacks, Expanded Abstracts, 62nd Annual Meeting of the Society of Exploration Geophysicists, New Orleans

Lawton, D.C., Yang, G.Y.C, Stewart, R.R., Potter, C.C., Uffen, J.D., and Boyd, J.D., 1997, Using 3C-3D seismic data to delineate a sandstone reservoir, Alberta, Canada: Expanded Abstracts, 67th Annual Meeting of the Society of Exploration Geophysicists, Dallas

Miller, S.L.M., Aydemir, E.O., and Margrave, G.F., 1995, Preliminary interpretation of P-P and P-S data from the Blackfoot broad-band survey: CREWES Project Research Report , **7**, Ch. 42.

Stewart, R., Ferguson, R., Miller, S., Gallant, E., and Margrave, G, 1996, The Blackfoot Seismic Experiments: Broad-band, 3C-3D, and 3D VSP surveys: CSEG Recorder, June.

Wood, J.M., and Hopkins, J.C., 1992, Traps associated with paleovalleys and interfluves in an unconformity bounded sequence: Lower Cretaceous Glauconitic Member, Southern Alberta, Canada: The American Association of Petroleum Geologists Bulletin, **76(6)**, 904-926.

FIGURES

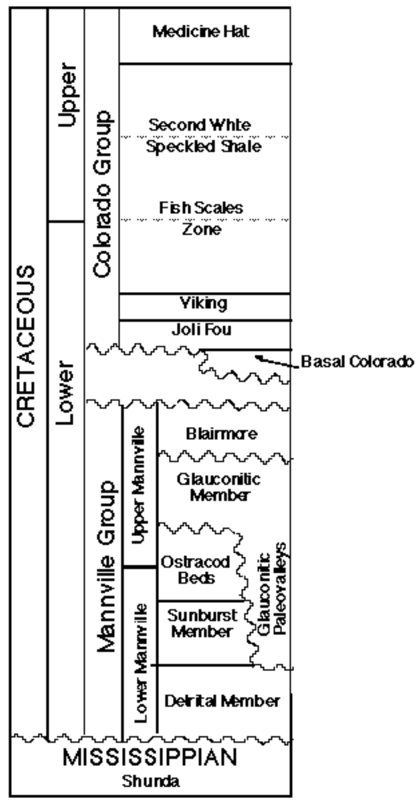

Fig. 1. Stratigraphic sequence for the Cretaceous unconformably atop the Mississippian. (After Wood and Hopkins, 1992)

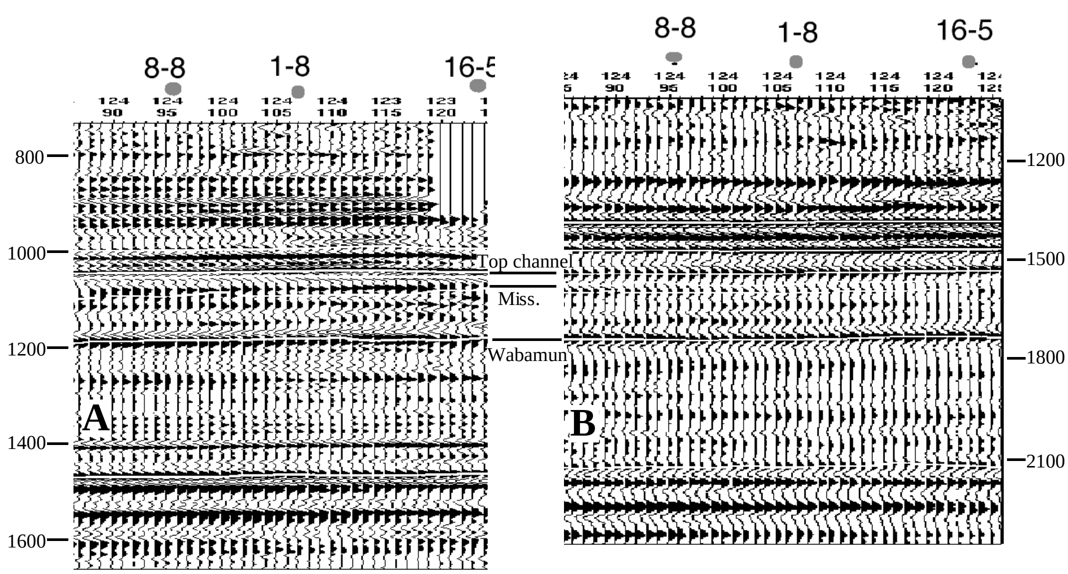

Fig. 2. Comparison of P-P (A) and P-S (B) final migrated sections. Top Channel, Mississippian, and Wabamun markers are approximately indicated.

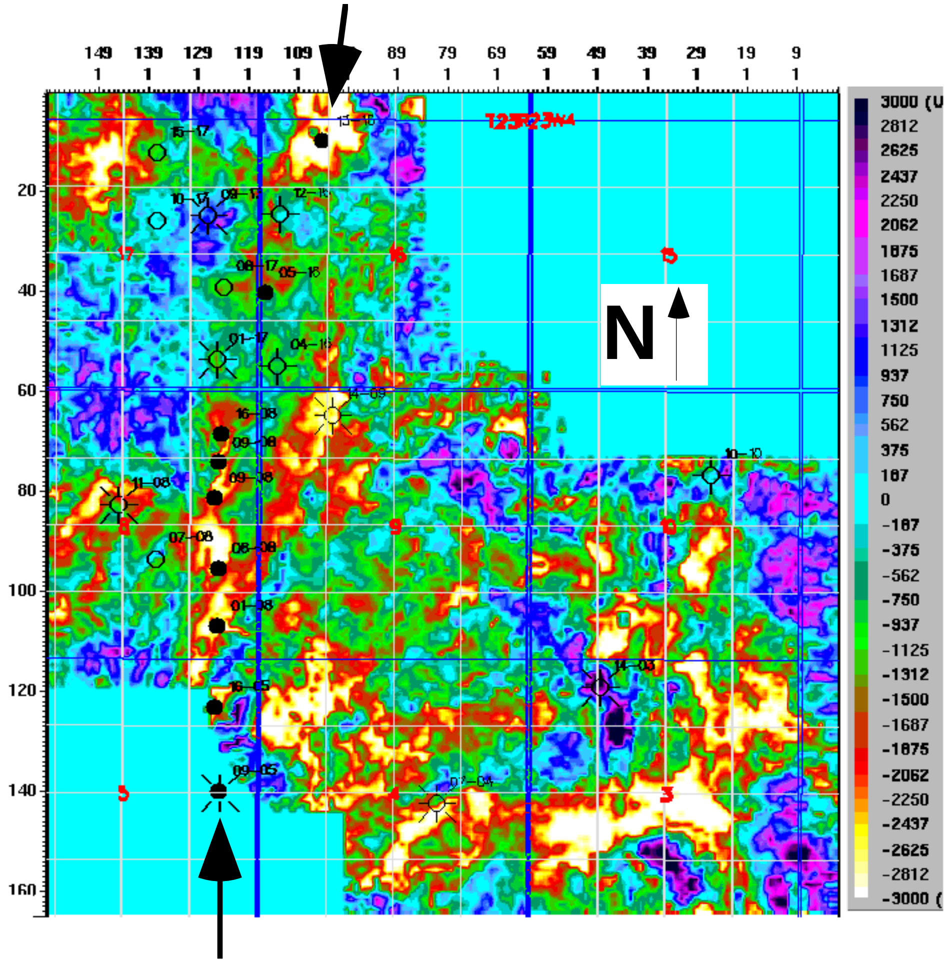

Fig. 3. P-P amplitude map through channel. Solid black dots are producing oil wells. Arrows indicate the approximate channel trend.

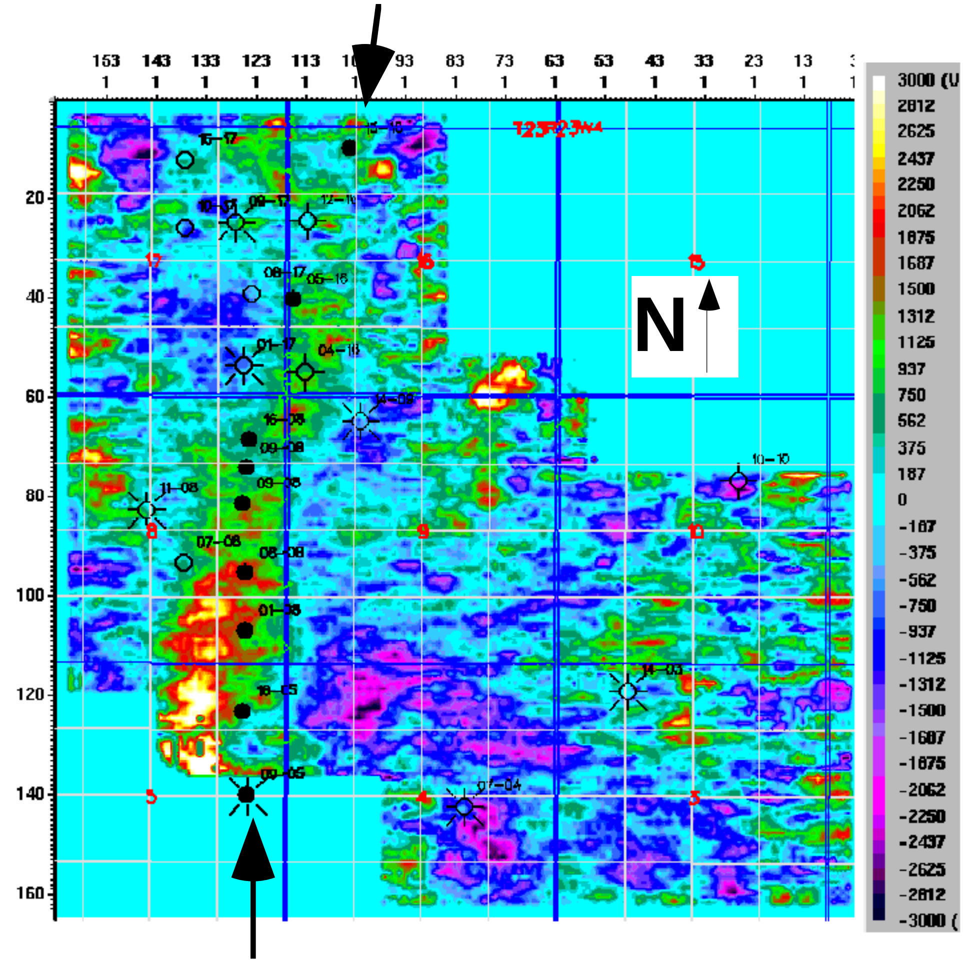

Fig. 4. P-S amplitude map through channel. Solid black dots are producing oil wells. Arrows indicate the approximate channel trend.

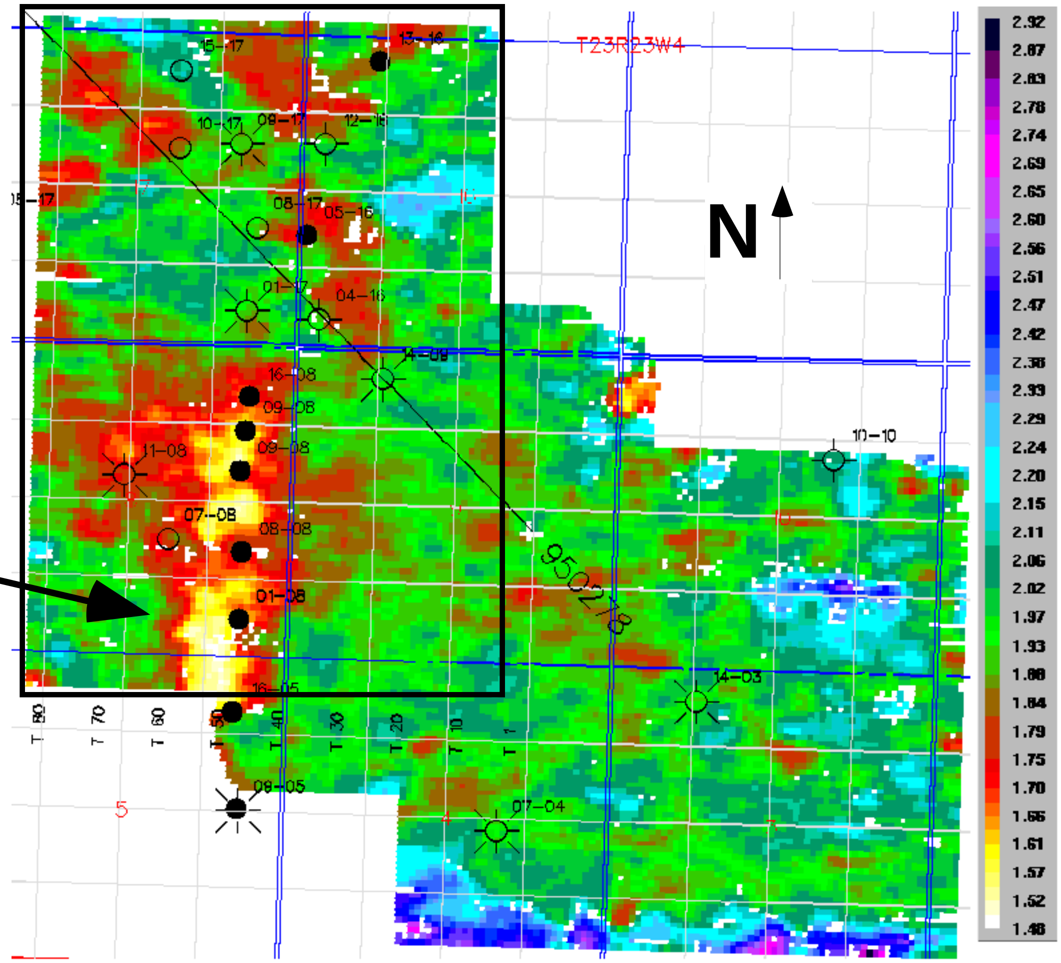

Fig. 5. Map of v_p/v_s ratio for the Channel-Wabamun interval. This was computed using P-P and P-S isochron maps over the Channel-Wabamun interval in equation 1. Solid black dots are producing oil wells. The arrow points to the center of the S-N trending anomaly and the rectangle indicates the extent of the images of Figure 6.

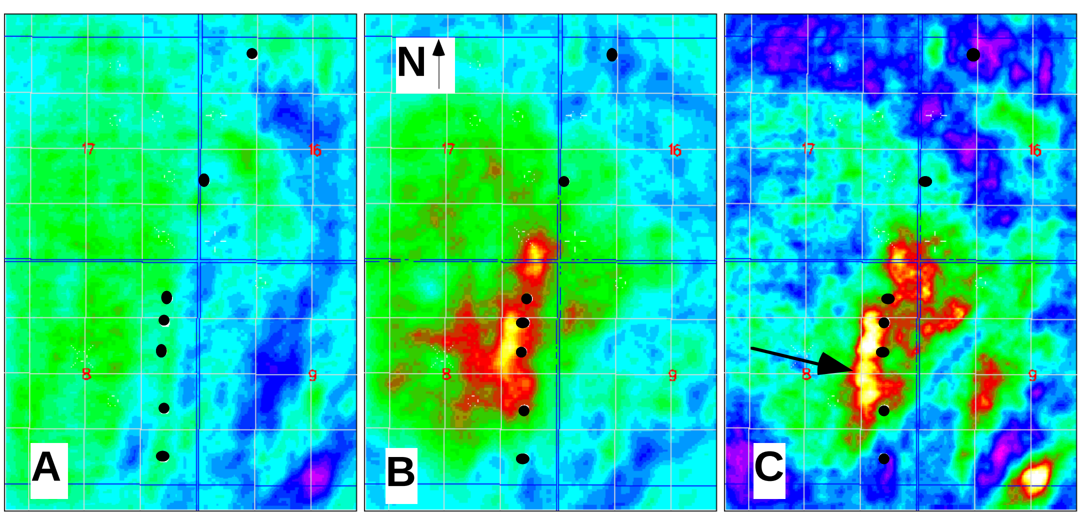

Fig. 6. P-P AVO display. Each image corresponds spatially to the box in Figure 5. A) A 3-D migration of a near offset stack of the P-P dataset. B) Similar to A) except that far offsets were used. C) Created by subtracting A) from B). Solid black dots are

producing oil wells and the arrow on C) denotes the anomaly to be compared to that in Figure 5.

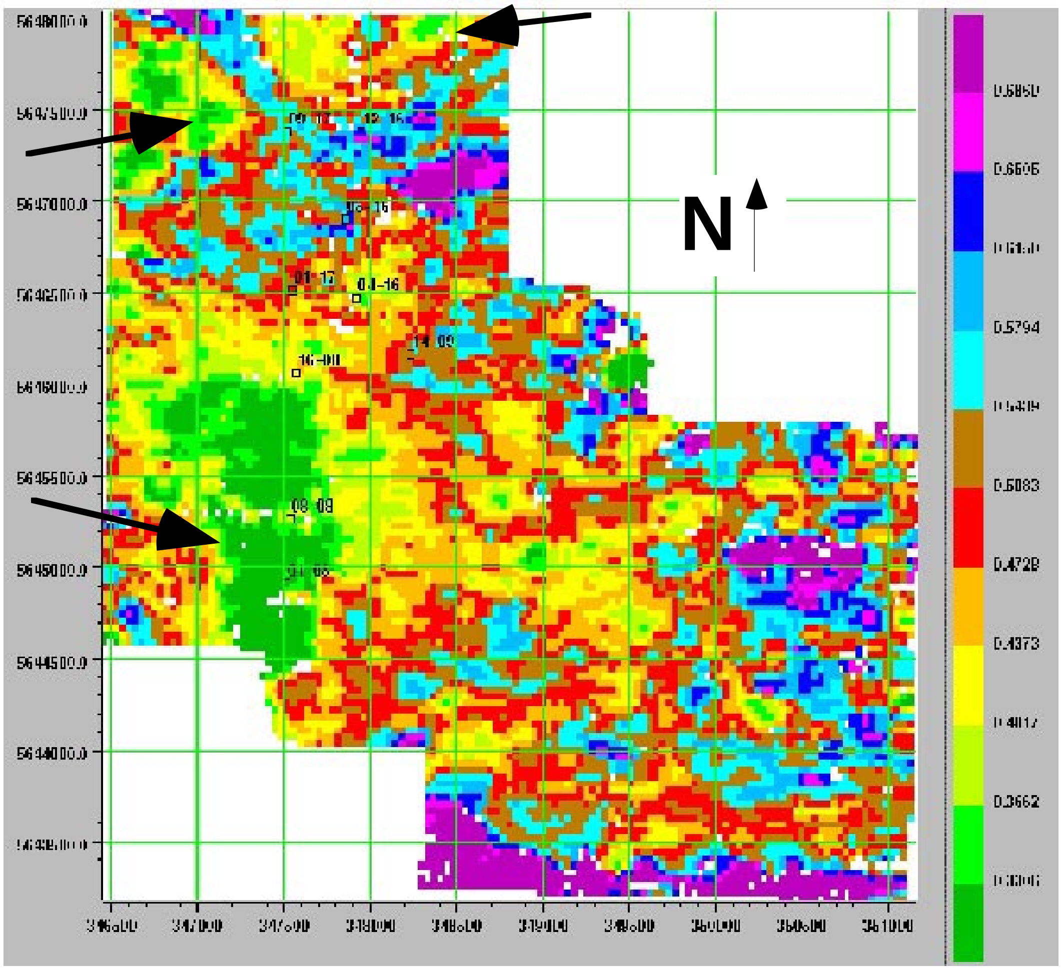

Fig. 7. A map of the fractional percentage of shale as estimated by cokriging using gamma ray log information (9 wells) and the v_p/v_s ratio map of figure 6. The arrows indicate the major predicted sand bodies.

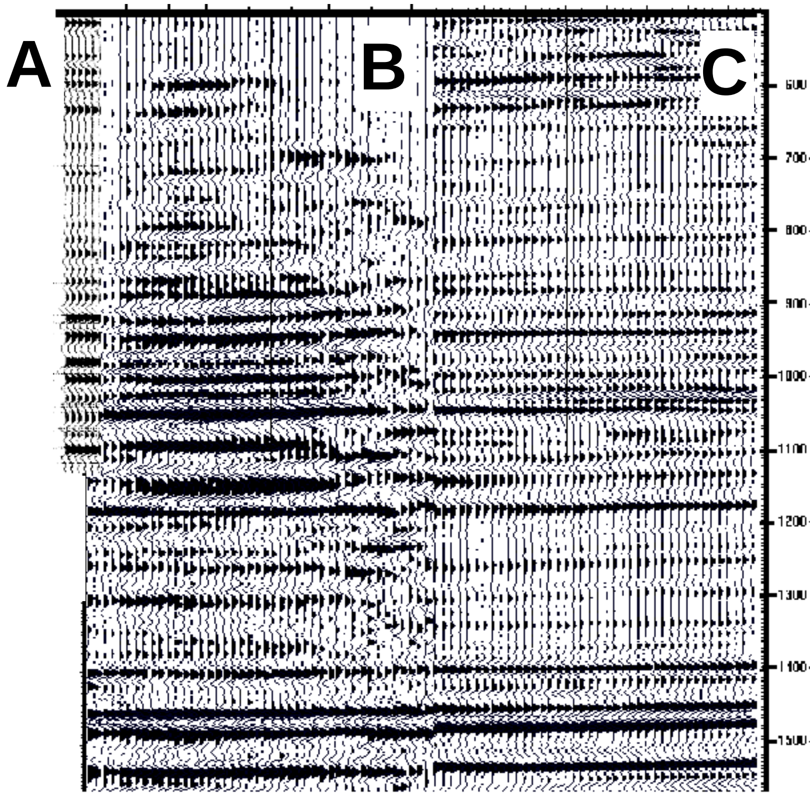

Fig. 8. A) A well log derived P-P synthetic seismogram. B) P-P data from the 3C-3D VSP. C) P-P data from the surface 3C-3D.